Chapter 4

Quantum Control

The attempt to control reactions has been the goal of many for thousands of years. Often the tactics used were what are termed passive control methods, methods such as changing concentration levels, pressure, and temperature. Quantum control uses a different tool for directing reaction paths. Since the advent of the first working laser by T.H. Maiman in the 1960's, laser radiation has been used to control microscopic processes such as bond cleavage and bond formation, taking advantage of its intense and small bandwidth properties. In a general sense the use of laser radiation defines a way of actively guiding chemical reactions on the microscopic level. For clarification the terms of passive and active control methods will be discussed.

The term passive control is nicely summed up by Rice and Zhao [84]. The information that passive control should convey is that i) the reactant molecules and solvent molecules are not subject to manipulation by external fields during the evolution to products, and therefore the reaction occurs under a field-free evolution of the reactants, ii) the evolution of the reactant molecules is largely incoherent, and iii) the reaction is initiated by an experimenter without controlling the evolution of the system at the level of molecular dynamics.

Bond-selective Excitation Along the lines of passive control, one of the first efforts to use laser radiation to control bond breakage, and perhaps the most obvious, was to radiate the molecular system with a tuned frequency of the laser which matches a local mode

of the molecule. Increasing the intensity of the laser radiation was thought to induce the bond-selective breakage. This way of control, also known as vibrationally mediated control, has been shown to be applicable to a few molecules such as HOOH [2], C_2HD [3], and HOD [4, 5]. This relative "simplistic" scheme of control, has had unfortunately relatively low success due to a phenomenon of energy redistribution which takes place on the picosecond time scale or even faster: Intramolecular Vibrational Redistribution (IVR). As the name indicates, the energy deposited by mode selective excitation flows to other modes of the molecule, typically before the bond breaks.

In contrast to passive techniques, active control attempts to guide the reaction at the molecular level by applying short bandwidth laser fields. Some of these techniques have shown that coherent effects, interference and time delays between laser pulses can be successful in controlling chemical reactions. This chapter intends to give an overview of the general methods of active control with insights to the experimental achievements. A division of the active schemes will also be applied to differentiate between those that operate under an iterative scheme and those that do not, starting with the latter.

4.1 General Schemes of Active Control

Phase-control In the scheme of phase-control, the coherence of laser radiation is exploited in order to control population transfer as well as the branching ratio for dissociation of small molecules [85]. The original Brumer-Shapiro scheme of coherent control [6] employs two phase-locked c.w. lasers with different frequencies. The first field emits a radiation frequency that is resonant with the ground state g and the final electronic state f, with a frequency of ω_1. The second field, which induces a multiphoton transition, has a frequency of ω_3, such that $\omega_1 = 3\omega_3$, as is seen in figure 4.1. Applying these two lasers to a molecular system leads to an interference term in the quantum mechanical description of the probability amplitudes of the wave function. The interference term can be manipulated by changing the phase of the two lasers, thereby controlling the branching ratio of different products. This method of control has been experimentally verified for the Hg atom [86], in which the population transfer to an atomic state was altered by varying the relative phases of two laser fields. The same approach has been used to control the branching ratios of dissociation for small molecules such as IBr [87] and HCl and CO [88, 89].

STIRAP The STImulated Raman scattering involving Adiabatic Passage, or STIRAP [9], is a control scheme designed to completely transfer population between specified quantum states, and is more robust to the fast oscillations than its pi-pulse counterpart, which is also used to invert the population [10, 90, 91, 92]. The basic version of the approach is shown in fig. 4.1 in which the inversion of population from the ground state g to the final state f is accomplished with the support of an intermediate state i. The design employs two intense laser pulses in order to achieve population inversion. Sequentially, the first pulse, the Stokes pulse, is resonant with the energy difference between the final state f and the intermediate state i. The second pulse is the pump pulse which couples the ground state g with the intermediate state i. This counter-intuitive sequence of pulses is designed such that when the pump pulse is switched on during the radiation with the Stokes pulse, a trapped state is produced which prevents populating the intermediate state, i. The population is considered to be virtually trapped or confined to the two states, g or f. The complete transfer from the ground to the final state occurs when the pump pulse is applied at the tail of the Stokes pulse. The phenomenon of trapping is a consequence of quantum interference between the two pathways leading to state i in fig. 4.1, i.e. the pathways induced via the pump and the Stokes pulses. Because the population does not occupy the intermediate state i, the method is especially attractive for systems where the intermediate state is plagued with decoherences or where population can be lost to other states. This technique of control has been experimentally verified for atoms and small molecules [9, 93, 94].

A new compounded control technique employs both the coherent control for its selectivity and the adiabatic passage for its robustness. The method, termed Coherent Controlled Adiabatic Passage, has been computationally demonstrated for controlling a double proton transfer in a model nucleotide base-pair with the goal of detecting and automatically repairing base-pair mutations [95].

Pump-Dump The scheme introduced by Tannor, Kosloff, and Rice in the 1980's is known as pump-dump or pump-control method [7, 8]. In contrast to the previous two methods which exploit quantum interference effects, this method is based on wavepacket dynamics and an appropriate time delay between pulses.

The model system presented by Tannor and Rice is best visualized using two electronic surfaces of a linear triatomic molecule: a model ABC molecule, see fig. 4.2. The left

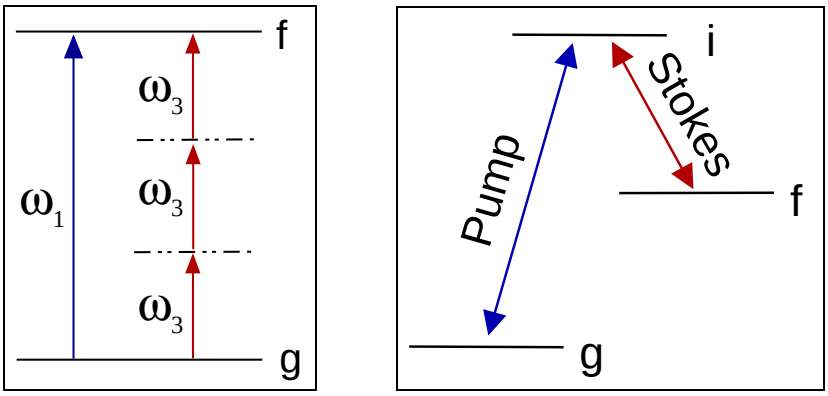

Coherent Control STIRAP

Figure 4.1: Two active control schemes: The left subfigure depicts a two c.w. laser pulse scheme where one pulse is resonant with a single photon ω_1 and the second resonant with three photons each with a frequency of ω_3. The main parameter which affects the control scheme is the relative phase of the two pulses. The second figure shows the STIRAP method of control, see text for details.

figure pictures the model ground electronic surface which contains a minimum and away from the equilibrium geometry the surface is dissociative along two different reaction pathways represented by the reaction given below.

$$\mathrm{A} + \mathrm{B} - \mathrm{C} \longleftarrow \mathrm{A} - \mathrm{B} - \mathrm{C} \longrightarrow \mathrm{A} - \mathrm{B} + \mathrm{C}$$

The modeled excited electronic surface, pictured on the right of fig. 4.2, is also characterized by a bound region which allows for evolution of the wavepacket, as indicated by the dashed curve, representing the wavepacket's trajectory.

The control mechanism will be discussed in terms of the original two-level model system. The initial wave function is located at the ground vibrational level in the ground electronic state. The first laser pulse, the pump pulse, transfers population from the ground state to the excited electronic state, where the wave function, no longer in a stationary state, begins to evolve along the path of steepest decent, in a way in which both bonds are stretched simultaneously. Due to the structure of the electronically excited state, the wavepacket moves in a complex way along the surface. The wavepacket's trajectory is traced on the excited state surface, see fig. 4.2. The trajectory could be superimposed directly onto the ground state and would indicate whether the wavepacket on the excited electronic state traverses the area directly above the dissociation channels on the ground electronic state. Based on the trajectory, the wavepacket enters this area depicted by the overlayed circle in

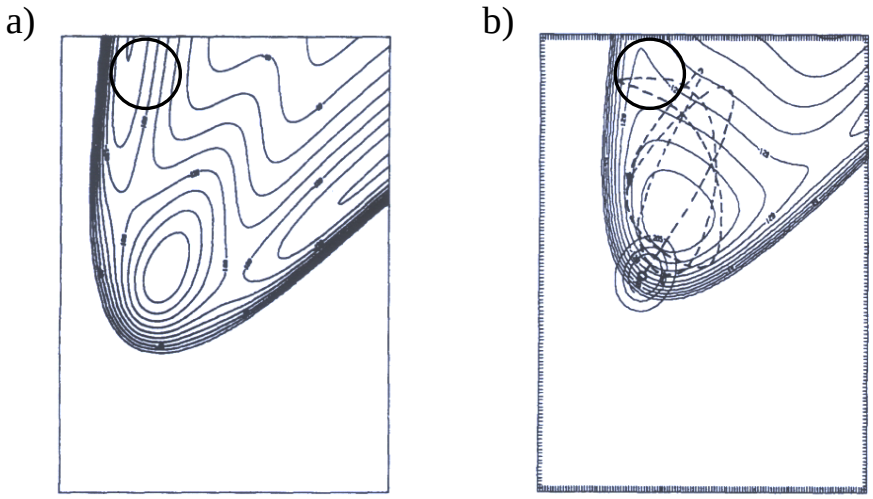

Figure 4.2: A contour plot of the a) modeled ground and b) excited electronic states used to exemplify the Pump-Dump control mechanism taken from [8]. Figure a) depicts the potential surface for the ground electronic state characterized by the two dissociation pathways. The potential in figure b) depicts the excited electronic state. The temporal evolution of the wavepacket is projected onto the contour plot of the electronic state.

fig. 4.2 and by applying a dump pulse at this moment in time the wavepacket is transferred into the dissocation channel, changing the molecule's dissociation pathway.

The pump-dump control scheme has been demonstrated experimentally on the diatomic sodium molecule, $\mathrm{Na_2}$ [96, 97] in which the branching ratio of $\mathrm{Na^+ + Na}$ to $\mathrm{Na_2^+}$ was modified. Zewail and researchers also applied this concept to the reaction $\mathrm{Xe + I_2 \rightarrow XeI + I}$ where an extra pump pulse was applied instead of a dump pulse, in a pump-pump approach [98, 99]. In this work, the approach of Tannor and Rice has also been extended to a more demanding three-level system of a large polyatomic organometallic molecule. Figure 4.3 depicts the general scheme already extended to a three-level system in which the pump pulse excites the initial wave function from the ground state, g to the intermediate excited state, i, and the dump pulse transfers population from the intermediate state, i, to the final state f. The well-timed dump pulse has placed the wavepacket selectively in the $\mathrm{A - B + C}$ dissociation channel.

Few-cycle Infra-red plus Ultraviolet (IR + UV) Another extension to the Tannor-Rice control method is a pump-pump via an infra-red (IR) and an ultraviolet (UV) laser pulse.

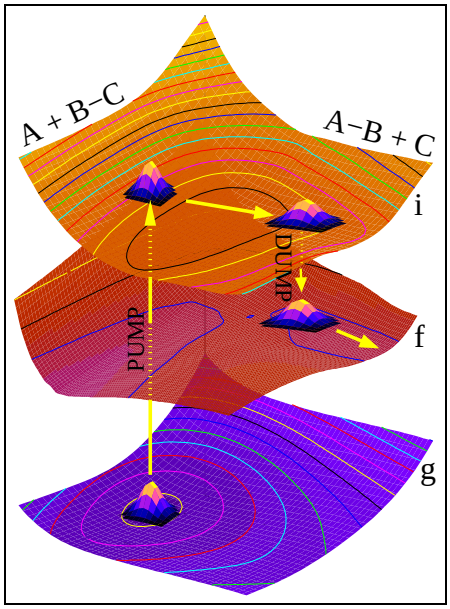

Figure 4.3: An extension of the pump-dump mechanism of Tannor-Rice to an electronic three-level system. Along several steps of the mechanism, a wavepacket is plotted to depict the actual motion. The mechanism entails two pulses, a pump and a dump pulse. The pump pulse transfers a portion of the ground state wave function to the highest-lying intermediate electronic state, i. The wavepacket evolves on the intermediate state where after some time it is located directly above a dissociation channel on the final electronic state, f. Applying a well-timed dump pulse, population is then transferred from the intermediate state to the dissociation channel on the final state, forming the products A-B + C.

The intent of this scheme is analogous to that of the pump-dump: laser control of chemical reactions via time delay between two pulses. In order to describe this approach, the general linear triatomic molecule $\mathrm{A}-\mathrm{B}-\mathrm{C}$ of the previous section will be adopted.

As the title suggests, this method employs two few-cycle laser pulses that can be used to control the photo-dissociation of a molecule. The first laser pulse, a few-cycle IR pulse, aims to create a vibrational wavepacket by exciting a superposition of vibrational eigenstates. A wavepacket is created which moves back and forth along the vibrational coordinates. At some instant in time, the wavepacket is localized below one of the two dissociation channels of the excited state, e.g. under the $\mathrm{A}+\mathrm{B}-\mathrm{C}$ channel. The few-cycle UV pulse is then applied, driving the localized wavepacket from the ground g to the final electronic state f. The electronic excitation via the UV pulse transfers population directly into this channel, producing the targeted products. A variation of this method, in which the UV pulse is applied to the wavepacket when the momentum favors a dissociation channel, has also successfully been applied [14].

The method of few-cycle IR + UV laser control has been applied to control selective dissociation of several systems, including the symmetric ozone molecule, in which the selective vibrational mode is attained via a many cycle IR laser pulse that occurs on the picosecond time scale [100], the symmetric FHF^- [13] molecule, and extended to asymmetric molecules HOD [14] and OHF^- [15].

Dynamic Stark Control The resulting Stark shifts of nonadiabatic potential energy curves due to intense nonresonant IR laser pulses have recently been exploited by Stolow *et al.* as a means in which control of molecular reactions can be achieved [101]. The coined term for this technique is Dynamic Stark Control (DSC).

The DSC method has been exemplified theoretically and experimentally for the IBr molecule [101]. The simulations incorporated three electronic states: the bound ground state, the first excited state which is slightly bound and leads to the formation of I+Br, and the second excited state, also slightly bound, leading to the formation of I+Br*. The two latter curves exhibit an avoided curve crossing. Initially the wavepacket is prepared on the second excited state, as it approaches the region near the avoided crossing, an ultra-short intense IR laser pulse is applied which shifts the curves to values lower in energy. A consequence of this shift is that the velocity of the wavepacket increases. Since the wavepacket's crossover is dependent on its velocity, the reaction will lead to more of the Br* product. In the same way, inducing the Stark shift at the initial time will shift and broaden the potential surfaces, so that when the wavepacket is transferred to the upper electronic state, the gradient is diminished, prohibiting the wavepacket from gaining much momentum. Therefore when the wavepacket approaches the potential crossings, it will be at a much slower velocity, thereby prefering the production of the Br product.

4.2 Iterative Active Control Schemes

Two schemes that apply iterative methods are Optimal Control Theory (OCT) and its experimental realization via closed-loop feedback control. The former will be discussed in general followed by a numerical iterative method for solving a set of coupled equations as introduced in reference [102]. The latter will be described in terms of the evolutionary algorithm which iteratively optimizes the laser pulse.

4.2.1 Optimal Control Theory (OCT)

Due to the anharmonicity of the excited state PES, the evolution of the wavepacket will, in most cases, spread out, preventing a clean dump into the wanted dissociation channel.

Tannor and Rice realized this limitation and included the optimization of the dump pulse, via OCT, in order to increase the selectivity of placing population into one of the two dissociation channels [7, 84]. The development of OCT has since been widely developed in order to produce tailored laser pulses which guide the wavepacket from its initial position to its predefined final position, the target state [16].

The standard version of OCT is based on the assumption that a molecular state, the target state $|\Psi_{\rm tar}\rangle$, is attainable by a laser driven molecular wave function $|\Psi(t)\rangle$ at time t_f. In other words, the overlap expression $|\langle\Psi_{\rm tar}|\Psi(t_f)\rangle|^2$ is equal to unity, [84, 85, 103]. To determine the laser pulse (the optimal pulse), which drives the system to its predefined target state, one considers the overlap to be a functional of the field strength $\mathbf{E}(t)$. An extremum of this functional should be obtained by the optimal pulse. To this end, OCT is formulated as a task which solves for the extremum with the constraint that the field strength has a finite value. The related control functional, is written as

$$J(t_f;\mathbf{E}) = |\langle\Psi_{\rm tar}|\Psi(t_f)\rangle|^2 - \frac{\lambda}{2}\int_{t_0}^{t_f} dt\ \frac{\mathbf{E}^2(t)}{s(t)}\ , \tag{4.1}$$

where the second term imposes a limit on the field strength via λ, the penalty function [84]. The first term determines the extent to which the control has been reached, and is known as the *control yield* $\mathcal{Q}$,

$$\mathcal{Q} = |\langle\Psi_{\rm tar}|\Psi(t_f)\rangle|^2. \tag{4.2}$$

The optimal control field is realizable by solving the extremum of the functional given in eq. 4.1; $\delta J(t_f;\mathbf{E})/\delta\mathbf{E}(t) = 0$. This results in the following expression for the optimal control field

$$\mathbf{E}(t) = \frac{s(t)i}{\lambda\hbar}\big(\langle\Theta(t)|\hat{\boldsymbol{\mu}}|\Psi(t)\rangle\langle\Psi(t_f)|\Psi_{\rm tar}\rangle + \langle\Psi_{\rm tar}|\Psi(t_f)\rangle\langle\Psi(t)|\hat{\boldsymbol{\mu}}|\Theta(t)\rangle\big), \tag{4.3}$$

where the shape function $s(t)$ has been introduced [104] and is given in eq. 3.39, and $\hat{\boldsymbol{\mu}}$, is the dipole operator given in eq. 3.35. The optimal control field is defined further by a forward propagated wave function $|\Psi(t)\rangle; t \equiv t_0 \longrightarrow t_f$ and a wave function that is propagated backward in time, $|\Theta(t)\rangle; t \equiv t_f \longrightarrow t_0$. The initial condition for the backward propagated wave function is $|\Theta(t_f)\rangle = |\Psi_{\rm tar}\rangle$, where the initial time is t_f since time runs in the reverse order. The calculation of the control field depends only on two functions, specifically the initial $|\Psi(t_0)\rangle$ and the final wave functions $|\Psi_{\rm tar}\rangle$ propagated forward and

backward in time respectively. The calculation of these wave functions depends simultaneously on the control field. The calculation of these terms are therefore coupled, and in order to solve for the control field an iterative scheme is typically employed. In the following, an iterative scheme will be presented for a two-level system.

Iterative Scheme for a Two-level System

This section aims to give a comprehensive overview of the iterative method applied to a two-level system, as suggest by Zhu, Botina and Rabitz [102], which is used to solve the set of coupled equations. The end effect of the iteration scheme is the production of the optimal control field: the field that drives an initial wave function $|\Psi_g(t_0)\rangle$, taken as the ground vibrational wave function on the ground electronic state, to a specified target state $|\Psi_f^{\mathrm{tar}}\rangle$ located completely on the final electronic excited state, i.e. $|\Psi_g^{\mathrm{tar}}\rangle = 0$. For clarity, a superscript is used to depict the iteration number on the control field and the wave functions. The scheme begins with an initial forward propagation that drives the ground state wave function to the excited state with a guessed laser field. The first iteration step actually begins with the first backward propagation and ends with the next forward propagation. Each of these processes will be described below.

Initial$^{(0)}$ *Forward Propagation*

The initial forward propagation of a wave function is accomplished by solving the time-dependent Schrödinger equation, eq. 3.1. Population is transferred between the ground g and the final excited electronic state f via laser-dipole-matter interaction, see section 3.1.3. The initial laser field, $\mathbf{E}^{(0)}(t)$, is a guess field defined by the user. Its purpose is to give a good starting point for the iterative process so that the pulse transfers at least a small portion of the initial wave function to the position of the target wave function. The iterative scheme requires the overlap at the final time to have a finite value not equal to zero $\langle\Psi_{\mathrm{tar}}|\Psi(t_f)\rangle \neq 0$, otherwise the control field will remain zero throughout the iteration process. The equations of motion are given below,

$$\begin{aligned} i\hbar\frac{\partial}{\partial t}|\Psi_g^{(0)}(t)\rangle &= \hat{\mathbf{H}}_g|\Psi_g^{(0)}(t)\rangle - \boldsymbol{\mu}_{gf}\mathbf{E}^{(0)}(t)|\Psi_f^{(0)}(t)\rangle \\ i\hbar\frac{\partial}{\partial t}|\Psi_f^{(0)}(t)\rangle &= \hat{\mathbf{H}}_f|\Psi_f^{(0)}(t)\rangle - \boldsymbol{\mu}_{fg}\mathbf{E}^{(0)}(t)|\Psi_g^{(0)}(t)\rangle \end{aligned} \tag{4.4}$$

where the nuclear Hamiltonian for the ground state $\hat{\mathbf{H}}_g$ and for the final state $\hat{\mathbf{H}}_f$ can be solved by applying the split operator technique given in eq. 3.44. The transition dipole moments are given as $\boldsymbol{\mu}_{gf}$ and $\boldsymbol{\mu}_{fg}$ which are considered to be equal. The wave functions are denoted as $|\Psi_g^{(0)}(t)\rangle$ and $|\Psi_f^{(0)}(t)\rangle$ for the ground and excited state respectively. The predefined electric field is given as

$$\mathbf{E}^{(0)}(t) = \mathbf{n}s(t)E_0\cos(\omega t), \tag{4.5}$$

where the shape function $s(t)$ is defined in equation 3.39, E_0 is the field amplitude and the cosine function contains the field frequency ω. The superscript$^{(0)}$ is used to denote the terms which are calculated from the initial forward propagation.

First*$^{(1)}$ *Backward Propagation: $t \equiv t_f \longrightarrow t_0$

The first backward propagation initiates the iterative process. In this step the control field is, for the first time, calculated by incorporating both the forward $|\Psi^{(0)}(t)\rangle$ and backward $|\Theta^{(1)}(t)\rangle$ wave functions of the previous and current iteration respectively. The initial condition for the backward wave propagation is given as $|\Theta_f(t_f)\rangle = |\Psi_f^{\mathrm{tar}}\rangle$ for the target state located on the final electronic state and $|\Theta_g(t_f)\rangle = |\Psi_g^{\mathrm{tar}}\rangle = 0$ for the target state located on the ground electronic state. Their temporal evolution is calculated by solving the following equations of motion,

$$\begin{aligned} i\hbar\frac{\partial}{\partial t}|\Theta_g^{(1)}(t)\rangle &= \hat{\mathbf{H}}_g|\Theta_g^{(1)}(t)\rangle - \boldsymbol{\mu}_{gf}\mathbf{E}^{(1b)}(t)|\Theta_f^{(1)}(t)\rangle \\ i\hbar\frac{\partial}{\partial t}|\Theta_f^{(1)}(t)\rangle &= \hat{\mathbf{H}}_f|\Theta_f^{(1)}(t)\rangle - \boldsymbol{\mu}_{fg}\mathbf{E}^{(1b)}(t)|\Theta_g^{(1)}(t)\rangle. \end{aligned} \tag{4.6}$$

The first term in eq. 4.6, defined by the nuclear Hamiltonian $\hat{\mathbf{H}}$, can be solved again by applying the split operator technique given in eq. 3.44, where Δt is now replaced with $-\Delta t$ to accommodate for the reversal of time. The control field is given as

$$\mathbf{E}^{(1b)}(t) = \frac{s(t)i}{\lambda\hbar}\big(\langle\Theta_g^{(1)}(t)|\hat{\boldsymbol{\mu}}|\Psi_f^{(0)}(t)\rangle\langle\Psi_f^{(0)}(t_f)|\Psi_f^{\mathrm{tar}}\rangle + \langle\Psi_f^{\mathrm{tar}}|\Psi_f^{(0)}(t_f)\rangle\langle\Psi_g^{(0)}(t)|\hat{\boldsymbol{\mu}}|\Theta_f^{(1)}(t)\rangle\big) \tag{4.7}$$

and is expressed in terms of the initial forward wave function $|\Psi^{(0)}(t)\rangle$, and the current backward wave function $|\Theta^{(1)}(t)\rangle$. The superscript $^{(1b)}$ is used to denote the first backward calculated electric field. It now becomes evident that the wave functions that were calculated in the set of eqs. 4.4 for the initial forward propagation must have been saved at every time step to be used in this current stage of the iteration process.

First*$^{(1)}$ *Forward Propagation: $t \equiv t_0 \longrightarrow t_f$

The first cycle of the iterative process is finalized upon the completion of the first forward propagation of the wave function. The initial wave function for this and subsequent forward propagations is the ground vibrational wave function of the ground electronic state, $|\Psi_g^{(n)}(t_0)\rangle = |\Psi_g(t_0)\rangle$, where n runs over the iteration steps. The equations of motion are given again for completion

$$\begin{aligned} i\hbar\frac{\partial}{\partial t}|\Psi_g^{(1)}(t)\rangle &= \hat{\mathbf{H}}_g|\Psi_g^{(1)}(t)\rangle - \boldsymbol{\mu}_{gf}\mathbf{E}^{(1f)}(t)|\Psi_f^{(1)}(t)\rangle \\ i\hbar\frac{\partial}{\partial t}|\Psi_f^{(1)}(t)\rangle &= \hat{\mathbf{H}}_f|\Psi_f^{(1)}(t)\rangle - \boldsymbol{\mu}_{fg}\mathbf{E}^{(1f)}(t)|\Psi_g^{(1)}(t)\rangle \end{aligned} \tag{4.8}$$

where the electric field is calculated as

$$\mathbf{E}^{(1f)}(t) = \frac{s(t)i}{\lambda\hbar}\big(\langle\Theta_g^{(1)}(t)|\hat{\boldsymbol{\mu}}|\Psi_f^{(1)}(t)\rangle\langle\Psi_f^{(1)}(t_f)|\Psi_f^{\mathrm{tar}}\rangle + \langle\Psi_f^{\mathrm{tar}}|\Psi_f^{(1)}(t_f)\rangle\langle\Psi_g^{(1)}(t)|\hat{\boldsymbol{\mu}}|\Theta_f^{(1)}(t)\rangle\big), \tag{4.9}$$

and is expressed in terms of the current forward wave function $|\Psi^{(1)}(t)\rangle$, and the previous backward wave function $|\Theta^{(1)}(t)\rangle$, calculated in eq. 4.6. The electric field is superscripted with $^{(1f)}$ to distinguish the calculated forward from the backward electric field. Again the electric field depends on the previous stage of the iteration process and therefore the backward wave functions in eq. 4.6 must have been saved at every time step. At this point in the iterative process the electric field $\mathbf{E}^{(1f)}(t)$, has already improved the control yield, see eq. 4.2, from that of the guess field. The final optimal control field is obtained when convergence has been reached.

The application of OCT on quantum molecular dynamics was initially developed and applied by Rabitz and co-workers [16, 102, 105]. The theory was extended to optimize the dump pulse for the Tannor-Rice control scheme in a two-level system [17]. The optimal electric fields that result from OCT simulations tend to be very complicated and are difficult to reproduce in the laboratory. For this reason experimentalists moved to a method of control where the optimal field is calculated using a closed-loop feedback strategy, which also tends to produce complex fields, and will be discussed shortly.

It should be mentioned that OCT is a method which, when applied to larger systems with many degrees of freedom, quickly becomes exhaustive. This is understood when one considers a simple one-dimensional two-level system with the following parameters: a grid of 128 points, propagation time of 150 fs with a time step of 0.01 fs. In such a

system, the wave function consists of a vector of 128 points for each state that has to be saved along every time step. This results in saving 128×2 values 15,000 times. Now consider an extension of this system to two-dimensions, then instead of saving a vector of 128 points, a matrix of 128×128 must be saved for every time step. It is clear by increasing the number of states and the number of dimensions that the iterative scheme applied to OCT quickly becomes computationally very demanding. One solution might be to program OCT in parallel or to apply a noniterative numerical scheme in order to solve the control field [106]. One can also apply local optimal control [17, 107, 108].

4.2.2 Closed-loop Feedback Experiments

The tailored electric fields that are produced from OCT simulations tend to be rather complex and therefore difficult to reproduce for experimentation. It was for this reason that Judson and Rabitz introduced a control scheme for the laboratory, in which the molecular dynamics are steered by improvements of the electric field in what is known as a closed-loop feedback experiment [18]. The basic components of such a scheme can be visualized in fig. 4.4, in which a laser source, a pulse shaper, a sample, a detection device, and a computer that contains the evolutionary algorithm are shown. The scheme in working order occurs as follows.

The laser source produces a short intense laser pulse which interacts with the sample. The products of the reaction are analyzed by a mass spectrometer where the signal is transferred to a computer and analyzed via an evolutionary algorithm. The modified form of the electric field, i.e. the phase and amplitude, produced by the evolutionary algorithm is sent to a pulse shaper where the new electric field is produced. The modified electric field interacts again with the molecular beam producing a different ratio of products which is fed back to the algorithm. Through this iterative or adaptive process, the algorithm typically produces a very flexible laser pulse that optimizes the predefined target products.

The evolutionary algorithm that modifies the electric field is based on three key concepts of biological evolution [109, 110, 111]. The first concept uses the individual's "fitness" as a criterion of whether or not its genes get transferred to the next generation. The second concept is that the offspring's genetics are based off the mixture from its parents, and are characterized by a crossover rate. The last main concept used is that of small mutations

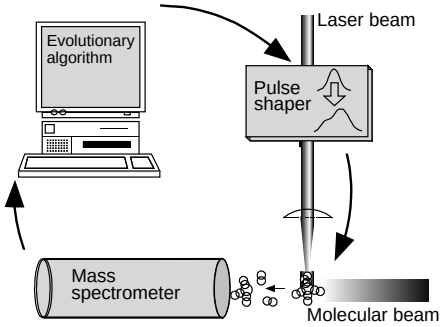

Figure 4.4: A schematic representation of the experimental setup for a closed-loop feedback experiment (taken from [19]). The femtosecond laser field interacts with the molecular beam where a reaction occurs. The products are recorded via the mass spectrometer and the signal is analyzed by a computer. The signal modifies the parameters in the pulse-shaper which eventually maximizes the control task.

that can make the genes of the offspring either more or less fit. Rabitz *et al.*, applied this algorithm to the control scheme to illustrate its efficiency in optimizing the rotational states of KCl [18]. This scheme has also been successfully applied to several large molecular systems [19, 112, 26], but as is often the case the electric field that is produced is very complex. In a dual effort between experiment and theory, the experimentally produced electric field can be deciphered. This has been accomplished by employing quantum dynamics on *ab initio* potential energy curves [27] as well as to modeled curves coupled to a bath [113] where just one degree of freedom was sufficient to decipher the experimentally achieved control pulse.

It should be noted that the search space used to find the optimal laser pulse in closed-loop feedback control experiments is gigantic. The search space is controlled by the number N of pixels in the pulse shaper which can modify both the amplitude A and phase P of the laser pulse and has a size of $(\mathrm{A}\times\mathrm{P})^N$. Binary Pulse Shaping (BPS) reduces the search space by neglecting the amplitude and limiting the phase to 0 or π, and results in a search space of 2^N. The advantage of BPS is that it allows for the visualization of the search space in a laser control experiment and has been applied to a multitude of problems [114].